tional target of the p53 family and responds to various apoptotic stimuli, including NGF withdrawal, our present results suggest that UNC5D is involved in NGF deprivation–induced PCD, which contributes to spontaneous regression of NB, and possibly developmentally regulated cell death of neural crest–derived neurons with NGF dependence. Identifying the more detailed signaling pathways may provide tools to develop novel therapeutic strategies against aggressive NBs, which are independent of NGF for cell growth and metastasis.

Methods

Patients and tumor samples. 108 fresh NB tumor tissues were obtained from patients who had been diagnosed between 1995 and 1999 in Japan. In all, 29 tumors were stage 1, 16 stage 2, 6 stage 4s, 36 stage 3, and 21 stage 4.

Cell culture, transfection, and RNAi. NB cell lines were cultured in RPMI medium. Other cells used in this study were grown in DMEM medium (Sigma-Aldrich) supplemented with 10% (v/v) FBS. Fugene HD (Roche) was used for cell transfections, following the manufacturer's instructions. siRNAs were obtained from Dharmacon.

Preparation of the UNC5D-specific antibody. To generate the UNC5D-specific antibody, rabbit antiserum was raised against the peptides (amino acids 937–956) of human UNC5D and purified with the affinity purification column by MBL Co. Ltd. Specificity of the antibody was confirmed by IB analysis.

Generation of Unc5d$^{-/-}$ mice and isolation of primary sympathetic neurons. The *Unc5d* targeting vector was constructed using a BAC clone isolated from a C57BL/6J mouse genomic library (RPCI-23, 372F8 clone; Invitrogen). The 6.5-kb EcoR V–Sma I fragment spanning upstream of the first exon of *Unc5d* was used as the long arm, and the 1.2-kb Pst I fragment in the first intron as the short arm. The 1.0-kb Sma I–Pst I fragment containing the first exon served as the targeted sequence. The targeted sequence was replaced by the *loxP-PGK-Neo-loxP* selection cassette including *PGK-DTA*. The targeting construct was linearized and electroporated into F1 mouse–derived (129/SvJ × C57BL/6J) ES cells. G418-resistant ES clones were screened by PCR and further verified with Southern blotting using both internal and external probes. Finally, 3 independent germline-transmitting chimeric mice were obtained and used after removing *PGK-Neo* by *cre* cRNA microinjection into the zygote.

Sympathetic neurons were obtained by enzymatic dissociation of SCG from P0 newborn mice. 3×10^3 cells/well were plated in 6-well dishes (Collagen Type IV cellware; BD Biosciences) in MEM supplemented with 10% (v/v) FBS, 2 mM uridine (Sigma-Aldrich), 2 mM fluorodeoxyuridine (Sigma-Aldrich), and 50 ng/ml mouse NGF (Harlan) for 5 days. Continuously, cells were cultured with or without 50 ng/ml NGF for the following 3 days and observed every 12 hours. In the NGF depletion group, 1% volume anti-NGF antiserum (Accurate Chemical & Scientific Corp.) was added to the medium.

Semiquantitative and quantitative RT-PCR analysis. Total RNA was prepared using an RNeasy mini kit (Qiagen) according to the manufacturer's protocol. See Supplemental Methods for details.

Immunofluorescence and immunohistochemistry. Frozen sections of NB clinical samples as well as cultured cells were fixed with 4% (w/v) formaldehyde and then incubated with the corresponding antibodies. Nuclei were stained with DAPI (Vector Laboratories). Cells were visualized under a Fluoview laser scanning confocal microscope (Olympus). NB tissue samples were obtained from the patients in stage 1 who had been found by mass screening at the age of 6 months and had favorable biological characteristics, including age less than 1 year, single copy of *MYCN*, and favorable histology. Histology of the tissues was shown by H&E staining.

Immunohistochemical analysis was carried out using paraffin-embedded tissues as described previously (55).

Apoptosis assay. Cell death was analyzed using the Trypan blue staining procedure (14). Apoptosis was monitored using an in situ cell death detection Kit (Roche). Nuclei were stained with DAPI.

For apoptosis assay of primary NB cells, cells were fixed in 4% (w/v) paraformaldehyde and stained with DAPI. Percent apoptotic nuclei was counted in 3 separate fields as described previously (56). For PC12 cells, cells were collected at each time point, and FACS analysis was carried out.

Colony formation assay and soft-agar assay. The colony formation assay and soft-agar assay were performed as described previously (57).

IP and IB. IP and IB were performed as described previously (57), using nuclear extracts or whole cell lysates. Whole cell lysates were prepared as described previously (25). See Supplemental Methods for details.

In vitro caspase cleavage assay. See Supplemental Methods and ref. 58.

Luciferase reporter assay. The luciferase reporter assay was conducted using a Dual-Luciferase Reporter Assay System (Promega) as described previously (57). pM-VP16 expression vector was used as a positive control.

Treatment of primary NB cells and PC12 cells with NGF. Primary NB cells were dissected from fresh NB tissues at 4°C, seeded at a density of $1–2 \times 10^5$ cells/well in a 6-well plate, and cultured in RPMI/OPI medium (Nissui Pharmaceutical) supplemented with 10% (v/v) FBS and antibiotics. PC12 cells were seeded at a density of 1×10^6 cells per 10-cm dish in DMEM medium supplemented with 5% (v/v) FBS and 10% (v/v) horse serum. NGF was added on the next day at a final concentration of 50 ng/ml. Primary cells were grown for 4 days, and PC12 cells for 6 days, with a change of medium containing NGF every 2–3 days. In the NGF withdrawal group, anti-NGF antibody was added at a final concentration of 0.1 μg/ml. The adherent primary NB cells were subjected to subsequent studies.

For knockdown experiments, PC12 cells were seeded at a density of 2×10^5 cells/well in collagen-coated 6-well plates. Accell siRNA against rat UNC5D (Dharmacon) was transduced into PC12 cells twice for long-term knockdown according to the manufacturer's protocol. Control Accell siRNA was used as a negative control. Cells were then subjected to NGF treatment.

Statistics. Statistical analysis was performed using Stata 6.0 software (Stata Corp.). 2-tailed Student's *t* test was used to explore possible associations between UNC5D expression and other factors. The distinction between high and low levels of *UNC5D* mRNA was based on the median value of the real-time PCR data (median value, 1.47; $P = 0.0032$), regardless of tumor stage, *MYCN* copy number, or survival. Kaplan-Meier survival curves were drawn, and survival distributions were compared using the log-rank test. Cox regression models were used to explore associations among UNC5D, age, *MYCN* copy number, TRKA, origin, and survival. A *P* value less than 0.05 was considered significant.

Study approval. Studies using clinical NB samples were approved by the Institutional Review Board of Chiba Cancer Center. Written informed consent was provided by the patients' parents. The Review Board for Animal Life Science of Chiba Cancer Center approved all animal experiments.

Acknowledgments

We thank Kohei Akazawa for statistical analysis, Hiroki Nagase for helpful discussion, and Takahiro Inoue for the *Unc5d*$^{-/-}$ mouse. This work was funded in part by a Grant-in-Aid from the Ministry of Health, Labor, and Welfare of Japan for the Third Term Comprehensive Control Research for Cancer; by a grant from Takeda Science Foundation; by the National Cancer Center Research and Development Fund; and by Grants-in-Aid for Scientific Research from the Ministry of Education, Culture, Sports, Science and Technology of Japan (JSPS KAKENHI grants 19591271, 24249061, 21591378, and 24591566).

Received for publication July 25, 2012, and accepted in revised form April 25, 2013.

Address correspondence to: Akira Nakagawara, Division of Biochemistry and Innovative Cancer Therapeutics and Children's Cancer Research Center, Chiba Cancer Center Research Institute, 666-1 Nitona-Chou, Chuo-Ku, Chiba-city, Chiba 260-8717, Japan. Phone: 81.43.264.5431; Fax: 81.43.265.4459; E-mail: akiranak@chiba-cc.jp.

Seiki Haraguchi's present address is: Animal Breeding and Reproduction Division, National Agriculture and Food Research Organization, Tsukuba, Japan.

1. D'Angio GJ, Evans AE, Koop CE. Special pattern of widespread neuroblastoma with a favourable prognosis. *Lancet.* 1971;1(7708):1046–1049.
2. Nakagawara A, et al. Association between high levels of expression of the TRK gene and favorable outcome in human neuroblastoma. *N Engl J Med.* 1993; 328(12):847–854.
3. Christiansen H, et al. Neuroblastoma: inverse relationship between expression of N-myc and NGF-r. *Oncogene.* 1990;5(3):437–440.
4. Nakagawara A, Azar CG, Scavarda NJ, Brodeur GM. Expression and function of TRK-B and BDNF in human neuroblastomas. *Mol Cell Biol.* 1994; 14(1):759–767.
5. Nakagawara A. The NGF story and neuroblastoma. *Med Pediatr Oncol.* 1998;31(2):113–115.
6. Aloyz RS, et al. p53 is essential for developmental neuron death as regulated by the TrkA and p75 neurotrophin receptors. *J Cell Biol.* 1998; 143(6):1691–1703.
7. Jacobs WB, et al. p63 is an essential proapoptotic protein during neural development. *Neuron.* 2005; 48(5):743–756.
8. Persengiev SP, Kondova II, Kilpatrick DL. E2F4 actively promotes the initiation and maintenance of nerve growth factor-induced cell differentiation. *Mol Cell Biol.* 1999;19(9):6048–6056.
9. O'Hare MJ, et al. Induction and modulation of cerebellar granule neuron death by E2F-1. *J Biol Chem.* 2000;275(33):25358–25364.
10. Lee S, et al. Neuronal apoptosis linked to EglN3 prolyl hydroxylase and familial pheochromocytoma genes: developmental culling and cancer. *Cancer Cell.* 2005;8(2):155–167.
11. Schlisio S, et al. The kinesin KIF1Bbeta acts downstream from EglN3 to induce apoptosis and is a potential 1p36 tumor suppressor. *Genes Dev.* 2008; 22(7):884–893.
12. Munirajan AK, et al. KIF1Bbeta functions as a haploinsufficient tumor suppressor gene mapped to chromosome 1p36.2 by inducing apoptotic cell death. *J Biol Chem.* 2008;283(36):24426–24434.
13. Bredesen DE, Mehlen P, Rabizadeh S. Receptors that mediate cellular dependence. *Cell Death Differ.* 2005;12(8):1031–1043.
14. Mehlen P, et al. The DCC gene product induces apoptosis by a mechanism requiring receptor proteolysis. *Nature.* 1998;395(6704):801–804.
15. Bordeaux MC, et al. The RET proto-oncogene induces apoptosis: a novel mechanism for Hirschsprung disease. *EMBO J.* 2000;19(15):4056–4063.
16. Llambi F, Causeret F, Bloch-Gallego E, Mehlen P. Netrin-1 acts as a survival factor via its receptors UNC5H and DCC. *EMBO J.* 2001;20(11):2715–2722.
17. Wang H, et al. A newly identified dependence receptor UNC5H4 is induced during DNA damage-mediated apoptosis and transcriptional target of tumor suppressor p53. *Biochem Biophys Res Commun.* 2008;370(4):594–598.
18. Thibert C, et al. Inhibition of neuroepithelial patched-induced apoptosis by sonic hedgehog. *Science.* 2003;301(5634):843–846.
19. Matsunaga E, et al. RGM and its receptor neogenin regulate neuronal survival. *Nat Cell Biol.* 2004; 6(8):749–755.
20. Mourali J, et al. Anaplastic lymphoma kinase is a dependence receptor whose proapoptotic functions are activated by caspase cleavage. *Mol Cell Biol.* 2006;26(16):6209–6222.
21. Stupack DG, et al. Apoptosis of adherent cells by recruitment of caspase-8 to unligated integrins. *J Cell Biol.* 2001;155(3):459–470.
22. Ohira M, et al. Expression profiling and characterization of 4200 genes cloned from primary neuroblastomas: identification of 305 genes differentially expressed between favorable and unfavorable subsets. *Oncogene.* 2003;22(35):5525–5536.
23. Mehlen P, Mazelin L. The dependence receptors DCC and UNC5H as a link between neuronal guidance and survival. *Biol Cell.* 2003;95(7):425–436.
24. Tanikawa C, Matsuda K, Fukuda S, Nakamura Y, Arakawa H. p53RDL1 regulates p53-dependent apoptosis. *Nat Cell Biol.* 2003;5(3):216–223.
25. Williams ME, et al. UNC5A promotes neuronal apoptosis during spinal cord development independent of netrin-1. *Nat Neurosci.* 2006;9(8):996–998.
26. Lu X, et al. The netrin receptor UNC5B mediates guidance events controlling morphogenesis of the vascular system. *Nature.* 2004;432(7014):179–186.
27. Przyborski SA, Knowles BB, Ackerman SL. Embryonic phenotype of Unc5h3 mutant mice suggests chemorepulsion during the formation of the rostral cerebellar boundary. *Development.* 1998; 125(1):41–50.
28. Deckwerth TL, et al. BAX is required for neuronal death after trophic factor deprivation and during development. *Neuron.* 1996;17(3):401–411.
29. Schroeter EH, Kisslinger JA, Kopan R. Notch-1 signalling requires ligand-induced proteolytic release of intracellular domain. *Nature.* 1998; 393(6683):382–386.
30. Kimberly WT, Zheng JB, Guenette SY, Selkoe DJ. The intracellular domain of the beta-amyloid precursor protein is stabilized by Fe65 and translocates to the nucleus in a notch-like manner. *J Biol Chem.* 2001;276(43):40288–40292.
31. Pediconi N, et al. Differential regulation of E2F1 apoptotic target genes in response to DNA damage. *Nat Cell Biol.* 2003;5(6):552–558.
32. Iaquinta PJ, Lees JA. Life and death decisions by the E2F transcription factors. *Curr Opin Cell Biol.* 2007; 19(6):649–657.
33. Johnson DG, Ohtani K, Nevins JR. Autoregulatory control of E2F1 expression in response to positive and negative regulators of cell cycle progression. *Genes Dev.* 1994;8(13):1514–1525.
34. Williams ME, Strickland P, Watanabe K, Hinck L. UNC5H1 induces apoptosis via its juxtamembrane region through an interaction with NRAGE. *J Biol Chem.* 2003;278(19):17483–17490.
35. Llambi F, et al. The dependence receptor UNC5H2 mediates apoptosis through DAP-kinase. *EMBO J.* 2005;24(6):1192–1201.
36. Sawada T, Hirayama M, Nakata T, Takeda T, Takasugi N, Mori T, Maeda K, Koide R, Hanawa Y, Tsunoda A, et al. Mass screening for neuroblastoma in infants in Japan. Interim report of a mass screening study group. *Lancet.* 1984;2(8397):271–273.
37. Woods WG, et al. A population-based study of the usefulness of screening for neuroblastoma. *Lancet.* 1996;348(9043):1682–1687.
38. Schilling FH, et al. Children may not benefit from neuroblastoma screening at 1 year of age. Updated results of the population based controlled trial in Germany. *Cancer Lett.* 2003;197(1–2):19–28.
39. Delloye-Bourgeois C, et al. Netrin-1 acts as a survival factor for aggressive neuroblastoma. *J Exp Med.* 2009;206(4):833–847.
40. Thiebault K, et al. The netrin-1 receptors UNC5H are putative tumor suppressors controlling cell death commitment. *Proc Natl Acad Sci U S A.* 2003; 100(7):4173–4178.
41. Payne SR, Kemp CJ. Tumor suppressor genetics. *Carcinogenesis.* 2005;26(12):2031–2045.
42. Huang J, et al. Down-regulation of SFRP1 as a putative tumor suppressor gene can contribute to human hepatocellular carcinoma. *BMC Cancer.* 2007;7:126.
43. Wu X, et al. HTPAP gene on chromosome 8p is a candidate metastasis suppressor for human hepatocellular carcinoma. *Oncogene.* 2006;25(12):1832–1840.
44. Seitz S, et al. Strong indication for a breast cancer susceptibility gene on chromosome 8p12-p22: linkage analysis in German breast cancer families. *Oncogene.* 1997;14(6):741–743.
45. Prasad MA, Trybus TM, Wojno KJ, Macoska JA. Homozygous and frequent deletion of proximal 8p sequences in human prostate cancers: identification of a potential tumor suppressor gene site. *Genes Chromosomes Cancer.* 1998;23(3):255–262.
46. Véronique GB, et al. Comprehensive profiling of 8p11-12 amplification in breast cancer. *Mol Cancer Res.* 2005;3(12):655–667.
47. Koed K, et al. High-density single nucleotide polymorphism array defines novel stage and location-dependent allelic imbalances in human bladder tumors. *Cancer Res.* 2005;65(1):34–45.
48. Rauch TA, et al. High-resolution mapping of DNA hypermethylation and hypomethylation in lung cancer. *Proc Natl Acad Sci U S A.* 2008;105(1):252–257.
49. Wells A, Marti U. Signalling shortcuts: cell-surface receptors in the nucleus? *Nat Rev Mol Cell Biol.* 2002; 3(9):697–702.
50. Johnson HM, Subramaniam PS, Olsnes S, Jans DA. Trafficking and signaling pathways of nuclear localizing protein ligands and their receptors. *Bioessays.* 2004;26(9):993–1004.
51. Taniguchi Y, Kim SH, Sisodia SS. Presenilin-dependent "gamma-secretase" processing of deleted in colorectal cancer (DCC). *J Biol Chem.* 2003; 278(33):30425–30428.
52. Troy CM, Shelanski ML. Caspase-2 redux. *Cell Death Differ.* 2003;10(1):101–107.
53. Troy CM, et al. Death in the balance: alternative participation of the caspase-2 and -9 pathways in neuronal death induced by nerve growth factor deprivation. *J Neurosci.* 2001;21(14):5007–5016.
54. Ianari A, et al. Proapoptotic function of the retinoblastoma tumor suppressor protein. *Cancer Cell.* 2009;15(3):184–194.
55. Ando K, et al. Expression of TSLC1, a candidate tumor suppressor gene mapped to chromosome 11q23, is downregulated in unfavorable neuroblastoma without promoter hypermethylation. *Int J Cancer.* 2008;123(9):2087–2094.
56. Stefanis L, Park DS, Friedman WJ, Greene LA. Caspase-dependent and -independent death of camptothecin-treated embryonic cortical neurons. *J Neurosci.* 1999;19(15):6235–6247.
57. Li Y, et al. A novel HECT-type E3 ubiquitin protein ligase NEDL1 enhances the p53-mediated apoptotic cell death in its catalytic activity-independent manner. *Oncogene.* 2008;27(26):3700–3709.
58. Foveau B, et al. Amplification of apoptosis through sequential caspase cleavage of the MET tyrosine kinase receptor. *Cell Death Differ.* 2007;14(4):752–764.

Journal of Human Genetics (2013) 58, 428–433

www.nature.com/jhg

REVIEW

Clinical application of the CpG island methylator phenotype to prognostic diagnosis in neuroblastomas

Kiyoshi Asada, Masanobu Abe and Toshikazu Ushijima

Clinical applications of aberrant DNA methylation to cancer diagnostics and therapeutics are accelerating. Especially, the CpG island methylator phenotype (CIMP), simultaneous methylation of multiple genes, provides information that cannot be obtained by other diagnostic methods and therapeutic opportunities. CIMP is known to be associated with poor or good prognosis depending upon cancer types. We identified that CIMP in neuroblastomas (NBLs) is strongly associated with poor prognosis in Japanese NBL cases (hazard ratio (HR) = 22). Almost all NBLs with *MYCN* amplification displayed CIMP, and even among NBLs without *MYCN* amplification, NBLs with CIMP had worse prognosis (HR = 12). The prognostic power was faithfully reproduced in German NBL cases by the same methods, and also in Italian and Swedish NBL cases with different analytical methods. Mechanistically, methylation silencing of different sets of tumor-suppressor genes is involved in poor prognosis of NBLs with CIMP, and the presence of CIMP is most sensitively detected by methylation of the *PCDHB* family. For therapeutic purposes, a combination of 5-aza-2′-deoxycytidine, a DNA-demethylating drug, with 13-*cis*-retinoic acid, a differentiating drug, has been shown to be effective for NBLs *in vitro*, and further development of a better combination(s) is awaited. Now, epigenetic diagnosis and therapeutics are becoming or have become an important choice for cancer patients.
Journal of Human Genetics (2013) **58,** 428–433; doi:10.1038/jhg.2013.64; published online 6 June 2013

Keywords: CIMP; neuroblastoma; poor prognosis

INTRODUCTION

Aberrant DNA methylation is inherited over cell divisions and is deeply involved in carcinogenesis. Increasing numbers of cancer-specific aberrant methylation have been identified, and their usefulness in cancer diagnostics is becoming clear. DNA-demethylating drugs have been developed, and their usefulness in cancer therapeutics is also becoming clear. In cancer diagnostics, methylation of the Septin-9 gene in plasma is now being clinically evaluated as a detection marker for colorectal cancers.[1] Methylation of O^6-methylguanine-DNA methyltransferase in glioblastoma tissues is also used to predict the response of tumors to alkylating drugs.[2] Methylation of glutathione *S*-transferase pi1 specific to prostate cancer cells is used to detect the presence of prostate cancer in prostatectomy or biopsy tissue.[3] In addition to methylation of specific genes, the CpG island methylator phenotype (CIMP), methylation of multiple genes, has been reported to be associated with prognosis in various cancers.[4]

The therapeutic application of DNA methylation has already been brought into practice. Two demethylating drugs, 5-aza-2′-deoxycytidine (5-aza-CdR) and 5-azacytidine (5-aza-CR), have been approved by the US Food and Drug Administration for treatment of myelodysplastic syndrome. Application of these demethylating drugs to treatment of solid tumors is being tested in clinical trials.[5] In addition to these clinically used drugs, a new generation of DNA-demethylating drugs, such as SGI-110 and CP-4200, are also being developed.[6] Combinations of DNA-demethylating drugs with other drugs, such as histone deacetylase inhibitors,[7] cellular differentiating drugs[8] and cytotoxic drugs,[9] have produced some promising results.

In this review, we will introduce CIMP in various cancers and then focus on the high usefulness of CIMP in prognostic diagnosis of neuroblastomas (NBLs) and the potential in their treatment.

CIMP IN VARIOUS CANCERS OTHER THAN NBLS

CIMP was originally established in colorectal cancers by the pioneering work of Toyota *et al*[10]. Some colorectal cancers had frequent DNA methylation of specific CpG islands and were associated with microsatellite instability. Colorectal cancers are now classified into three groups, CIMP-high (CIMP1, HME), CIMP-low (CIMP2, IME) and CIMP-0 (CIMP-negative, LME), using tumor-specific methylation markers.[11–13] CIMP-high cases show low mortality compared with CIMP-0 (hazard ratio (HR) = 0.44; 95% confidence interval (CI) = 0.22–0.88; $n = 649$)[11] (Table 1). CIMP-high, -low and -0 are strongly associated with mutations of *BRAF*, *KRAS* and *TP53*, respectively.[11,12] Although the cause–consequence relationship between oncogene mutations and CIMP has not been established, some investigators propose that methylation silencing of senescence pathways is necessary to suppress oncogene-induced senescence and for a cell with an oncogene mutation to survive.[14,15]

Division of Epigenomics, National Cancer Center Research Institute, Tokyo, Japan
Correspondence: Dr T Ushijima, Division of Epigenomics, National Cancer Center Research Institute, 1-1 Tsukiji 5-chome, Chuo-ku, Tokyo 104-0045, Japan.
E-mail: tushijim@ncc.go.jp
Received 24 April 2013; revised 6 May 2013; accepted 11 May 2013; published online 6 June 2013

Table 1 CIMP in various cancers and association with prognosis

	CIMP markers			
Cancer type	*Original markers*	*Other markers*	*Prognosis of patients with CIMP*	*Reference*
Colorectal cancer	MINT27, MINT2, MINT1, MINT12, MINT17, MINT31, MINT25	None	NA	10
Colorectal cancer	None	*CACNA1G, IGF2, NEUROG1, RUNX3, SOCS1*	NA	50
Colorectal cancer	MINT27, MINT2, MINT1, MINT12, MINT17, MINT31	*p16, p16ex1, hMLH1, RASSF1A, DAPK, MGMT, TIMP3, ER, sFRP1, MyoD1, HPP1, hTERT, RIZ1, p14, Megalin, COX2, THBS1, THBS2, SOCS1, RUNX3, Neurog1*	NA	12
Colorectal cancer	None	*p16, hMLH1, CACNA1G, IGF2, NEUROG1, RUNX3, SOCS1, CRABP1*	Good CIMP-high vs -0 (HR = 0.44; 95% CI = 0.22–0.88; $n = 649$)	11
Colorectal cancer	MINT2, MINT1, MINT17, MINT31,	*p16, hMLH1, RASSF1A, MGMT, TIMP3, p14, CACNA1G, IGF2, NEUROG1, RUNX3, SOCS1, ALX4, RASSF5, ABTB2, C4orf31, CHFR, COL4A2, DUSP26, EFEMP1, IGFBP3, IGFBP7, IRF8, LOX, PPP1R3C, SCAM1, STOX2, TLE4, TMEFF2, UCHL1, ADAMTS1, AOX1, CDO1, CLDN23, EDIL3, EFHD1, ELMO1, EPHB1, FBN2, HAND1, ID4, KIAA0495, PENK, PPP1R14A, SSFRP1, SLC30A10, SPON1, THBD, TSPYL5, ZNF447, BNIP3, CIDEB, DFNA5, GRHL2, HLTF, OVOL1, RASSF2, TOLLIP*	NA	13
Gastric cancer	MINT2, MINT1, MINT12, MINT31, MINT25	None	Good CIMP-high vs -negative, $P = 0.004$; CIMP-low vs -negative, $P = 0.012$; $n = 78$[25]	16,17,25
Lung cancer	MINT1, MINT31, MINT32	*p16, MLH1, RASSF1A, RARβ, APC, DAPK, MGMT, GSTP1, CDH1, CDH13, sFRP1, sFRP2, sFRP4, sFRP5, TMS1, LAMC2*	NA	18
Liver cancer	MINT2, MINT1, MINT27, MINT31	*p16, CACNA1G, COX2, ER*	NA	19
Ovarian cancer	None	182 CGIs on a CGI microarray	Poor $P < 0.001$, $n = 19$	24
Leukemia	None	*p16, DAPK, CDH1, CDH13, sFRP1, sFRP2, sFRP4, sFRP5, TMS1, FHIT, ADAMTS1, ADAMTS5, APAF1, ASPP1, DBC1, DIABLO, DKK3, HDPR1, hRFC, LATS1, LATS2, NES1, p14, p15, p57, p73, PACRG, PARK2, PTEN, REPRIMO, RIZ, SHP1, SMC1L1, SMC1L2, SYK, WIF1*	Poor $P = 0.04$, $n = 54$	21
Bladder cancer	None	*p16, RASSF1A, RARβ, APC, DAPK, MGMT, GSTP1, CDH1, CDH13, FHIT*	Poor $P = 0.01$, $n = 98$	22
Esophageal adenocarcinoma	None	*p16, APC, DAPK, MGMT, CDH1, TIMP3, ER*	Poor HR = 2.7; 95% CI = 1.1–6.5; $P = 0.02$; $n = 41$	23
Glioblastoma	None	1503 CpG sites on Infinium HumanMethylation450 bead array	Good $P = 0.017$, $n = 253$	26
Glioblastoma	None	9711 CpG sites on Infinium HumanMethylation450 bead array	Good $P < 0.001$, $n = 72$	27

Abbreviations: CI, confidence interval; CIMP, CpG island methylator phenotype; HR, hazard ratio; NA, not applicable.

The presence of CIMP has been reported in several other cancers, such as gastric,[16,17] lung,[18] liver,[19] ovarian cancers[20] and leukemias[21] (Table 1). The definition of CIMP is different in each cancer and the relationship between CIMP and prognosis is also different. Poor survival is associated with CIMP in bladder cancers ($P = 0.01$, $n = 98$),[22] esophageal adenocarcinomas (HR = 2.7; 95% CI = 1.1–6.5; $P = 0.02$; $n = 41$),[23] ovarian tumors ($P < 0.001$, $n = 19$)[24] and leukemias ($P = 0.04$, $n = 54$).[21] On the other hand, better survival is associated with CIMP in gastric cancers (CIMP-high vs -negative, $P = 0.004$, CIMP-low vs -negative, $P = 0.012$, $n = 78$).[25]

CIMP in glioblastomas is exceptionally well-characterized from a molecular viewpoint, and designated as G-CIMP. G-CIMP is associated with good prognosis ($P = 0.017$, $n = 253$),[26] and is known to be caused by isocitrate dehydrogenase 1 (*IDH1*) mutation.[27] Functionally, *IDH1* mutation has been shown as a gain-of-function mutation and to catalyze the NADPH-dependent reduction of α-ketoglutarate to 2-hydroxyglutarate.[28] 2-Hydroxyglutarate inhibits TET methylcytosine dioxygenase 2 that catalyzes the conversion of 5-methylcytosine to 5-hydroxymethylcytosine,[29] and the inhibition of TET is considered to lead to methylation of multiple genes. Similar to the association of *IDH1* mutation and G-CIMP, *IDH1/2* mutation is also associated with methylation patterns in AML.[30]

IDENTIFICATION OF CIMP IN NBLS AS A STRONG PROGNOSTIC MARKER

NBL, derived from primitive cells of the sympathetic nervous system, is the most frequent extracranial cancer in childhood,[31] and is characterized by two extreme outcomes, spontaneous regression and

rapid progression. Accurate risk prediction is important for NBL in order to implement a necessary and sufficient level of treatment, and the International Neuroblastoma Risk Group classification system has been established for this purpose.[32] In this system, seven prognostic factors (stage, age, histologic category, grade of tumor differentiation, DNA ploidy and copy-number status at *MYCN* and at chromosome 11q) are used as the most clinically relevant factors. However, especially in the NBLs without *MYCN* amplification, it is still difficult to predict accurate prognosis and to decide on the therapeutic strategy.

Considering the major involvement of epigenetic machinery in embryonic development,[33,34] we searched for CGIs specifically methylated in NBLs with poor prognosis, not in those with good prognosis, using methylation-sensitive representational difference analysis.[35] Five CGI (or CGI groups), namely the *PCDHB* family, the *PCDHA* family, *HLP*, *DKFZp451I127* and *CYP26C1*, were found to be specifically methylated in NBLs with poor prognosis. Methylation of these five CGI (groups) was dependent upon each other, and conformed to the concept of CIMP. Methylation levels of the *PCDHB* family showed a clear bimodal distribution (Figure 1a), and NBL cases with high methylation levels of the *PCDHB* family showed poor overall survival with a HR of 22 (95% CI = 5.3–93) in 140 Japanese NBL cases.[35] Therefore, we decided to use the methylation levels of the *PCDHB* family as a marker of CIMP in NBLs.

To avoid false 'too good' results likely to be obtained by a genome-wide screening, we analyzed the prognostic power of CIMP in 152 German NBL cases in collaboration with Dr Schwab and Dr Westermann[36] (Figure 1b). DNA of German NBL cases was sent to our laboratory in Tokyo without clinical information, and methylation levels of the *PCDHB* family were analyzed. Regarding the cutoff value, as values between 40 and 60% gave high HRs in Japanese NBL cases, cases with methylation levels lower than 40% and higher than 60% were classified as NBLs without and with CIMP, respectively. The strong association between CIMP and poor overall survival was faithfully reproduced in German NBL cases with a HR of 9.5 (95% CI = 3.2–28). In addition, German NBL cases had information on disease-free survival, which was not available in Japanese NBL cases, and CIMP was shown to have prognostic significance also for disease-free survival with a HR of 5.4 (95% CI = 2.9–10). In addition to our studies, the strong prognostic power of CIMP was further confirmed in Italian and Swedish NBL cases.[37,38] Currently, in order to evaluate the clinical utility of CIMP as a prognostic marker, a prospective study is being conducted.

COMPARISON OF CIMP WITH *MYCN* AMPLIFICATION

MYCN amplification is known as the strongest prognostic marker for NBLs and is one of the first molecular markers used in practice.[39–41] The presence of *MYCN* amplification is therefore used as a biomarker for stratification of NBLs in practice and trials. Importantly, almost all NBLs with *MYCN* amplification displayed CIMP (37/38 in Japanese and 23/23 in German NBL cases) while some NBLs without *MYCN* amplification also displayed CIMP[35,36] (Figure 2a). The cases with *MYCN* amplification showed poor overall survival with HR of 9.5

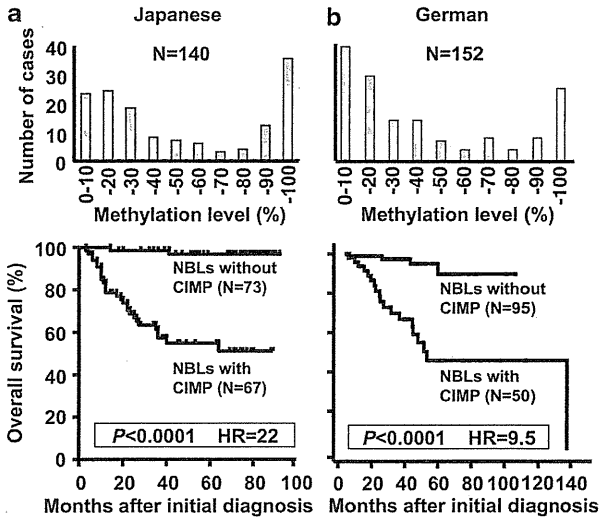

Figure 1 Bimodal distribution of methylation levels of the *PCDHB* family and its association with survival. (**a**) In 140 Japanese neuroblastoma (NBL) cases, the methylation level of the *PCDHB* family showed bimodal distribution (modified from Abe *et al.*[35]). The cutoff value for *PCDHB* family was set at 40%. NBLs with CpG island methylator phenotype (CIMP) had significantly and markedly worse overall survival, analyzed by the Kaplan–Meier method. (**b**) In 152 German NBL cases, a similar bimodal distribution of the *PCDHB* family methylation level was observed. As cutoff values between 40 and 60% gave high HRs in Japanese NBL cases, before the analysis, cutoff values of 40 and 60% were set for cases without and with CIMP, respectively, and cases with intermediate values were classified as intermediate. It was reproduced that NBLs with CIMP had significantly and markedly worse overall survival (modified from Abe *et al.*[36]).

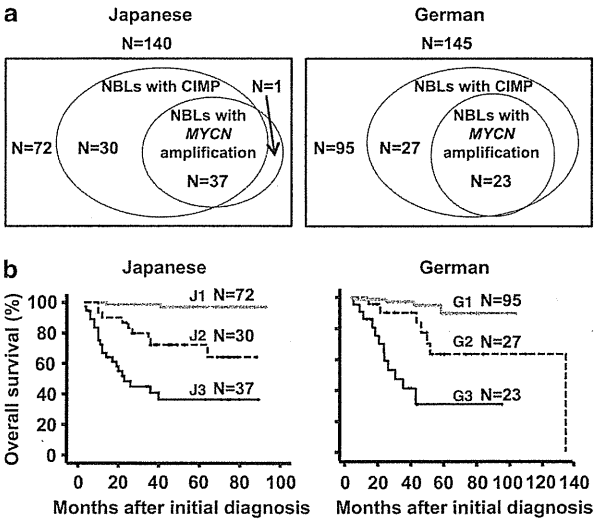

Figure 2 Comparison of CpG island methylator phenotype (CIMP) and *MYCN* amplification. (**a**) The relationship between neuroblastomas (NBLs) with CIMP and those with *MYCN* amplification are shown by Venn diagrams. Almost all NBLs with *MYCN* amplification (37/38 in Japanese and 23/23 in German NBL cases) displayed CIMP, and some additional cases had CIMP only. (**b**) Kaplan–Meier analysis of (J1, G1) NBL cases without CIMP or *MYCN* amplification ($N=72$ in Japanese and $N=95$ in German NBL cases), (J2, G2) NBL cases with CIMP without *MYCN* amplification ($N=30$ in Japanese and $N=27$ in German NBL cases), (J3, G3) NBL cases with both CIMP and *MYCN* amplification ($N=37$ in Japanese and $N=23$ in German NBL cases). Among NBLs without *MYCN* amplification (J1, J2 in Japanese and G1, G2 in German NBL cases), CIMP also had a significant and strong prognostic marker with a hazard ratio of 12 (95% confidence interval (CI) = 2.6–59; $P=0.002$) in Japanese and 4.5 (95% CI = 1.3–16; $P=0.02$) in German NBL cases.

(95% CI = 4.4–21) and 12 (95% CI = 4.9–29) in Japanese and German NBL cases, respectively.[35,36] Therefore, NBL cases were classified into three groups: (J1) NBL cases without CIMP nor *MYCN* amplification ($N = 72$), (J2) NBL cases with CIMP without *MYCN* amplification ($N = 30$) and (J3) NBL cases with both CIMP and *MYCN* amplification ($N = 37$) in Japanese NBL cases. German NBL cases were also classified into three groups (G1–G3) in the same manner (Figure 2b). The three groups, respectively, showed step-wise increases of risk, and notably, among NBLs without *MYCN* amplification (J1, J2 in Japanese and G1, G2 in German NBL cases), NBLs with CIMP showed worse prognosis with a HR of 12 (95% CI = 2.6–59) in Japanese and 4.5 (95% CI = 1.3–16) in German NBL cases. The almost complete inclusion of NBLs with *MYCN* amplification in those with CIMP indicates that these two abnormalities are very closely associated with each other. However, it is still unknown whether CIMP causes *MYCN* amplification, *MYCN* amplification causes CIMP, these two must coexist for development of NBLs, or if there is a shared upstream event.

MECHANISM FOR THE ASSOCIATION BETWEEN CIMP AND POOR PROGNOSIS

CGIs of the *PCDHB* family are located in their gene body, and their methylation was not associated with gene expression levels.[35] This suggested that, although methylation of the *PCDHB* family was closely associated with poor survival, simultaneous methylation of promoter CGIs was mechanistically involved in the poor survival (Figure 3). Indeed, in our study of Japanese NBL cases, methylation of promoter CGIs of the *RASSF1A*, *BLU*, *CYP26C1*, *FERD3L*, *CRYBA2* and *PCDHGC4* were methylated at significantly higher incidences in NBLs with CIMP, indicating that methylation silencing of tumor-suppressor genes was indeed associated with CIMP.[8,35]

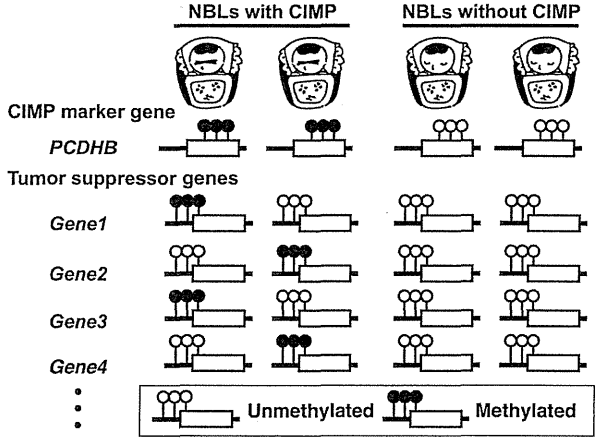

Figure 3 A likely mechanism for the association between CpG island methylator phenotype (CIMP) and poor prognosis. In neuroblastomas (NBLs) with and without CIMP, the exonic CGIs of the *PCDHB* family and promoter CGIs of tumor-suppressor genes typically showed methylation statuses as in this scheme. NBLs with CIMP had methylation of the exonic CGIs of the *PCDHB* family consistently, and that of promoter CGIs of multiple tumor-suppressor genes with lower frequencies. Although methylation silencing of tumor-suppressor genes was considered to be responsible for the poor prognosis of NBLs with CIMP, methylation of individual genes had less sensitivity of CIMP than methylation of the *PCDHB* family. On the other hand, NBLs without CIMP did not have methylation of the exonic CGIs of the *PCDHB* family or that of promoter CGIs of tumor-suppressor genes, and thus were considered to have a good prognosis.

To strengthen this hypothesis, we further analyzed methylation of promoter CGIs of genes whose silencing was reported to be involved in development or progression of NBLs, namely *CASP8*, *EMP3*, *HOXA9*, *NR1I2* and *CD44*. *CASP8* is an anti-apoptotic gene, and its methylation was reported to be associated with poor survival with HR of 5.3 ($P = 0.008$).[42] Also, methylation of *EMP3*, *HOXA9*, *NR1I2* and *CD44* were associated with poor survival with a *P*-value of 0.014, 0.03, 0.04 and 0.049, respectively.[42–45] We found that CIMP was associated with methylation of multiple promoter CGIs, mainly *CASP8* and *NR1I2*, but had stronger prognostic power than methylation of individual genes.[46] These results strengthened the hypothesis that CIMP leads to poor prognosis by induction of methylation of promoter CGIs of various tumor-suppressor genes at low incidences.

CIMP AS A POTENTIAL TARGET OF EPIGENETIC THERAPY

Poor prognosis of NBLs with CIMP is likely to be caused by silencing of multiple genes due to methylation of their promoter CGIs. As silenced genes are multiple and variable among individual NBLs, it was hypothesized that simultaneous demethylation of multiple genes could be effective for treatment of NBLs (Figure 4). Indeed, treatment of NBL cell lines with a demethylating drug, 5-aza-CdR, enhanced the sensitivity to the differentiation effect by 13-*cis*-retinoic acid.[8]

In addition to CIMP, aberrant histone modifications or modifying enzymes are also emerging as potential therapeutic targets of NBLs. For example, lysine-specific demethylase 1 (LSD1), a histone H3 lysine4 (H3K4) demethylase, is highly expressed in poorly differentiated NBLs, and inhibition of LSD1 using a monoamine oxidase inhibitor, tranylcypromine, resulted in growth suppression of NBLs *in vitro* and *in vivo*.[47] To improve selectivity for LSD1 over monoamine oxidase inhibitor, LSD1-selective inhibitors were developed,[48] and they are expected to show high anticancer efficacy and low toxicity in normal cells.

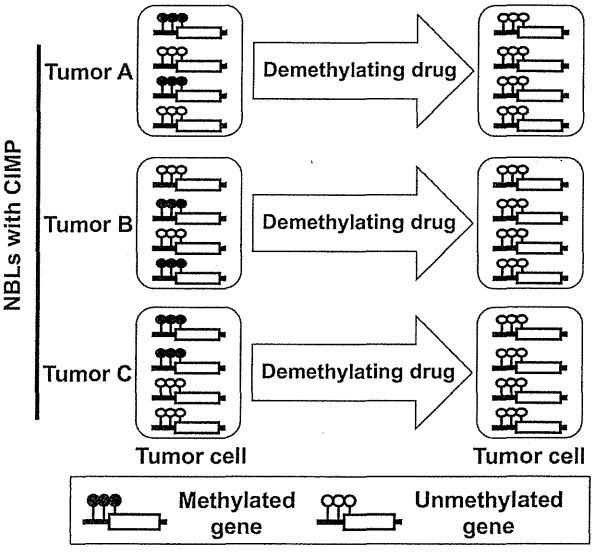

Figure 4 The concept of demethylating drug treatment for neuroblastomas (NBLs). In individual NBLs (tumor A–C), multiple but different tumor-suppressor genes are methylation-silenced, and reversal of these individual genes is difficult. By the use of a demethylating drug, multiple tumor-suppressor genes become simultaneously demethylated, and NBL cells are expected to show better responses to differentiation and cytotoxic agents.

Clinically, a phase I study of 5-aza-CdR with doxorubicin and cyclophosphamide in children with NBLs and other solid tumors was conducted in the United States,[49] and low-dose 5-aza-CdR ($5\,mg\,m^{-2}$) turned out to have tolerable toxicity in children. However, doses of 5-aza-CdR capable of producing clinically relevant biologic effects were not well tolerated. Different combinations between 5-aza-CdR and other drugs, such as differentiating drugs (13-*cis*-retinoic acid) or other epigenetic drugs (LSD1 inhibitors and histone deacetylase inhibitors), could improve the effectiveness of the demethylating drug for NBLs.

CONCLUSIONS

The usefulness of aberrant DNA methylation in cancer diagnostics and therapeutics is now coming into practice. In NBLs, CIMP has prognostic power in cases without *MYCN* amplification, and its strong prognostic power was validated in German, Italian and Swedish NBL cases. Combinations of a DNA-demethylating drug with a differentiating drug has been shown to be effective for NBLs with CIMP *in vitro*, and the appropriate dose and appropriate combination is expected to improve survival of NBL cases. Epigenetic diagnosis and therapeutics are becoming or have become an important choice for cancer patients.

CONFLICT OF INTEREST

The authors declare no conflict of interest.

ACKNOWLEDGEMENTS

This study was supported by Grants-in-Aid for the Third-Term Cancer Control Strategy Program from the Ministry of Health, Labour and Welfare, Japan, and by the National Cancer Center Research and Development Fund, Japan.

1 Church, T. R., Wandell, M., Lofton-Day, C., Mongin, S. J., Burger, M., Payne, S. R. *et al.* Prospective evaluation of methylated SEPT9 in plasma for detection of asymptomatic colorectal cancer. *Gut* in press (2013).
2 Hegi, M. E., Diserens, A. C., Gorlia, T., Hamou, M. F., de Tribolet, N., Weller, M. *et al.* MGMT gene silencing and benefit from temozolomide in glioblastoma. *N. Engl. J. Med.* **352,** 997–1003 (2005).
3 Van Neste, L., Herman, J. G., Otto, G., Bigley, J. W., Epstein, J. I. & Van Criekinge, W. The epigenetic promise for prostate cancer diagnosis. *Prostate* **72,** 1248–1261 (2011).
4 Teodoridis, J. M., Hardie, C. & Brown, R. CpG island methylator phenotype (CIMP) in cancer: causes and implications. *Cancer Lett.* **268,** 177–186 (2008).
5 Cowan, L. A., Talwar, S., Yang, A. S. & Will, D. N. A. Methylation inhibitors work in solid tumors? A review of the clinical experience with azacitidine and decitabine in solid tumors. *Epigenomics* **2,** 71–86 (2010).
6 Foulks, J. M., Parnell, K. M., Nix, R. N., Chau, S., Swierczek, K., Saunders, M. *et al.* Epigenetic drug discovery: targeting DNA methyltransferases. *J. Biomol. Screen.* **17,** 2–17 (2012).
7 Juergens, R. A., Wrangle, J., Vendetti, F. P., Murphy, S. C., Zhao, M., Coleman, B. *et al.* Combination epigenetic therapy has efficacy in patients with refractory advanced non-small cell lung cancer. *Cancer Discov.* **1,** 598–607 (2011).
8 Abe, M., Watanabe, N., McDonell, N., Takato, T., Ohira, M., Nakagawara, A. *et al.* Identification of genes targeted by CpG island methylator phenotype in neuroblastomas, and their possible integrative involvement in poor prognosis. *Oncology* **74,** 50–60 (2008).
9 Matei, D., Fang, F., Shen, C., Schilder, J., Arnold, A., Zeng, Y. *et al.* Epigenetic resensitization to platinum in ovarian cancer. *Cancer Res.* **72,** 2197–2205 (2012).
10 Toyota, M., Ahuja, N., Ohe-Toyota, M., Herman, J. G., Baylin, S. B. & Issa, J. P. CpG island methylator phenotype in colorectal cancer. *Proc. Natl Acad. Sci. USA* **96,** 8681–8686 (1999).
11 Ogino, S., Nosho, K., Kirkner, G. J., Kawasaki, T., Meyerhardt, J. A., Loda, M. *et al.* CpG island methylator phenotype, microsatellite instability, BRAF mutation and clinical outcome in colon cancer. *Gut* **58,** 90–96 (2009).
12 Shen, L., Toyota, M., Kondo, Y., Lin, E., Zhang, L., Guo, Y. *et al.* Integrated genetic and epigenetic analysis identifies three different subclasses of colon cancer. *Proc. Natl Acad. Sci. USA* **104,** 18654–18659 (2007).
13 Yagi, K., Akagi, K., Hayashi, H., Nagae, G., Tsuji, S., Isagawa, T. *et al.* Three DNA methylation epigenotypes in human colorectal cancer. *Clin. Cancer Res.* **16,** 21–33 (2010).
14 Suzuki, H., Igarashi, S., Nojima, M., Maruyama, R., Yamamoto, E., Kai, M. *et al.* IGFBP7 is a p53-responsive gene specifically silenced in colorectal cancer with CpG island methylator phenotype. *Carcinogenesis* **31,** 342–349 (2010).
15 Hinoue, T., Weisenberger, D. J., Pan, F., Campan, M., Kim, M., Young, J. *et al.* Analysis of the association between CIMP and BRAF in colorectal cancer by DNA methylation profiling. *PLoS One* **4,** e8357 (2009).
16 Kim, H., Kim, Y. H., Kim, S. E., Kim, N. G. & Noh, S. H. Concerted promoter hypermethylation of hMLH1, p16INK4A, and E-cadherin in gastric carcinomas with microsatellite instability. *J. Pathol.* **200,** 23–31 (2003).
17 Toyota, M., Ahuja, N., Suzuki, H., Itoh, F., Ohe-Toyota, M., Imai, K. *et al.* Aberrant methylation in gastric cancer associated with the CpG island methylator phenotype. *Cancer Res.* **59,** 5438–5442 (1999).
18 Marsit, C. J., Houseman, E. A., Christensen, B. C., Eddy, K., Bueno, R., Sugarbaker, D. J. *et al.* Examination of a CpG island methylator phenotype and implications of methylation profiles in solid tumors. *Cancer Res.* **66,** 10621–10629 (2006).
19 Shen, L., Ahuja, N., Shen, Y., Habib, N. A., Toyota, M., Rashid, A. *et al.* DNA methylation and environmental exposures in human hepatocellular carcinoma. *J. Natl Cancer Inst.* **94,** 755–761 (2002).
20 Strathdee, G., Appleton, K., Illand, M., Millan, D. W., Sargent, J., Paul, J. *et al.* Primary ovarian carcinomas display multiple methylator phenotypes involving known tumor suppressor genes. *Am. J. Pathol.* **158,** 1121–1127 (2001).
21 Roman-Gomez, J., Jimenez-Velasco, A., Agirre, X., Castillejo, J. A., Navarro, G., Calasanz, M. J. *et al.* CpG island methylator phenotype redefines the prognostic effect of t(12;21) in childhood acute lymphoblastic leukemia. *Clin. Cancer Res.* **12,** 4845–4850 (2006).
22 Maruyama, R., Toyooka, S., Toyooka, K. O., Harada, K., Virmani, A. K., Zochbauer-Muller, S. *et al.* Aberrant promoter methylation profile of bladder cancer and its relationship to clinicopathological features. *Cancer Res.* **61,** 8659–8663 (2001).
23 Brock, M. V., Gou, M., Akiyama, Y., Muller, A., Wu, T. T., Montgomery, E. *et al.* Prognostic importance of promoter hypermethylation of multiple genes in esophageal adenocarcinoma. *Clin. Cancer Res.* **9,** 2912–2919 (2003).
24 Wei, S. H., Chen, C. M., Strathdee, G., Harnsomburana, J., Shyu, C. R., Rahmatpanah, F. *et al.* Methylation microarray analysis of late-stage ovarian carcinomas distinguishes progression-free survival in patients and identifies candidate epigenetic markers. *Clin. Cancer Res.* **8,** 2246–2252 (2002).
25 Kusano, M., Toyota, M., Suzuki, H., Akino, K., Aoki, F., Fujita, M. *et al.* Genetic, epigenetic, and clinicopathologic features of gastric carcinomas with the CpG island methylator phenotype and an association with Epstein-Barr virus. *Cancer* **106,** 1467–1479 (2006).
26 Noushmehr, H., Weisenberger, D. J., Diefes, K., Phillips, H. S., Pujara, K., Berman, B. P. *et al.* Identification of a CpG island methylator phenotype that defines a distinct subgroup of glioma. *Cancer Cell* **17,** 510–522 (2010).
27 Turcan, S., Rohle, D., Goenka, A., Walsh, L. A., Fang, F., Yilmaz, E. *et al.* IDH1 mutation is sufficient to establish the glioma hypermethylator phenotype. *Nature* **483,** 479–483 (2012).
28 Dang, L., White, D. W., Gross, S., Bennett, B. D., Bittinger, M. A., Driggers, E. M. *et al.* Cancer-associated IDH1 mutations produce 2-hydroxyglutarate. *Nature* **462,** 739–744 (2009).
29 Xu, W., Yang, H., Liu, Y., Yang, Y., Wang, P., Kim, S. H. *et al.* Oncometabolite 2-hydroxyglutarate is a competitive inhibitor of alpha-ketoglutarate-dependent dioxygenases. *Cancer Cell* **19,** 17–30 (2011).
30 Figueroa, M. E., Abdel-Wahab, O., Lu, C., Ward, P. S., Patel, J., Shih, A. *et al.* Leukemic IDH1 and IDH2 mutations result in a hypermethylation phenotype, disrupt TET2 function, and impair hematopoietic differentiation. *Cancer Cell* **18,** 553–567 (2010).
31 Maris, J. M. Recent advances in neuroblastoma. *N. Engl. J. Med.* **362,** 2202–2211 (2010).
32 Cohn, S. L., Pearson, A. D., London, W. B., Monclair, T., Ambros, P. F., Brodeur, G. M. *et al.* The International Neuroblastoma Risk Group (INRG) classification system: an INRG Task Force report. *J. Clin. Oncol.* **27,** 289–297 (2009).
33 Jaenisch, R. & Bird, A. Epigenetic regulation of gene expression: how the genome integrates intrinsic and environmental signals. *Nat. Genet.* **33** (Suppl), 245–254 (2003).
34 Li, E. Chromatin modification and epigenetic reprogramming in mammalian development. *Nat. Rev. Genet.* **3,** 662–673 (2002).
35 Abe, M., Ohira, M., Kaneda, A., Yagi, Y., Yamamoto, S., Kitano, Y. *et al.* CpG island methylator phenotype is a strong determinant of poor prognosis in neuroblastomas. *Cancer Res.* **65,** 828–834 (2005).
36 Abe, M., Westermann, F., Nakagawara, A., Takato, T., Schwab, M. & Ushijima, T. Marked and independent prognostic significance of the CpG island methylator phenotype in neuroblastomas. *Cancer Lett.* **247,** 253–258 (2007).
37 Banelli, B., Brigati, C., Di Vinci, A., Casciano, I., Forlani, A., Borzi, L. *et al.* A pyrosequencing assay for the quantitative methylation analysis of the PCDHB gene cluster, the major factor in neuroblastoma methylator phenotype. *Lab. Invest.* **92,** 458–465 (2011).
38 Kiss, N. B., Kogner, P., Johnsen, J. I., Martinsson, T., Larsson, C. & Geli, J. Quantitative global and gene-specific promoter methylation in relation to biological properties of neuroblastomas. *BMC Med. Genet.* **13,** 83 (2012).
39 Schwab, M., Alitalo, K., Klempnauer, K. H., Varmus, H. E., Bishop, J. M., Gilbert, F. *et al.* Amplified DNA with limited homology to myc cellular oncogene is shared by human neuroblastoma cell lines and a neuroblastoma tumour. *Nature* **305,** 245–248 (1983).

40 Brodeur, G. M., Seeger, R. C., Schwab, M., Varmus, H. E. & Bishop, J. M. Amplification of N-myc in untreated human neuroblastomas correlates with advanced disease stage. *Science* **224,** 1121–1124 (1984).
41 Seeger, R. C., Brodeur, G. M., Sather, H., Dalton, A., Siegel, S. E., Wong, K. Y. *et al.* Association of multiple copies of the N-myc oncogene with rapid progression of neuroblastomas. *N. Engl. J. Med.* **313,** 1111–1116 (1985).
42 Grau, E., Martinez, F., Orellana, C., Canete, A., Yanez, Y., Oltra, S. *et al.* Hypermethylation of apoptotic genes as independent prognostic factor in neuroblastoma disease. *Mol. Carcinog.* **50,** 153–162 (2011).
43 Alaminos, M., Davalos, V., Ropero, S., Setien, F., Paz, M. F., Herranz, M. *et al.* EMP3, a myelin-related gene located in the critical 19q13.3 region, is epigenetically silenced and exhibits features of a candidate tumor suppressor in glioma and neuroblastoma. *Cancer Res.* **65,** 2565–2571 (2005).
44 Alaminos, M., Davalos, V., Cheung, N. K., Gerald, W. L. & Esteller, M. Clustering of gene hypermethylation associated with clinical risk groups in neuroblastoma. *J. Natl Cancer Inst.* **96,** 1208–1219 (2004).
45 Misawa, A., Inoue, J., Sugino, Y., Hosoi, H., Sugimoto, T., Hosoda, F. *et al.* Methylation-associated silencing of the nuclear receptor 1I2 gene in advanced-type neuroblastomas, identified by bacterial artificial chromosome array-based methylated CpG island amplification. *Cancer Res.* **65,** 10233–10242 (2005).
46 Asada, K., Watanabe, N., Nakamura, Y., Ohira, M., Westermann, F., Scwab, M. *et al.* Stronger prognostic power of the CpG island methylator phenotype than methylation of individual genes in neuroblastomas. *Jpn J. Clin. Oncol.* in press (2013).
47 Schulte, J. H., Lim, S., Schramm, A., Friedrichs, N., Koster, J., Versteeg, R. *et al.* Lysine-specific demethylase 1 is strongly expressed in poorly differentiated neuroblastoma: implications for therapy. *Cancer Res.* **69,** 2065–2071 (2009).
48 Ueda, R., Suzuki, T., Mino, K., Tsumoto, H., Nakagawa, H., Hasegawa, M. *et al.* Identification of cell-active lysine specific demethylase 1-selective inhibitors. *J. Am. Chem. Soc.* **131,** 17536–17537 (2009).
49 George, R. E., Lahti, J. M., Adamson, P. C., Zhu, K., Finkelstein, D., Ingle, A. M. *et al.* Phase I study of decitabine with doxorubicin and cyclophosphamide in children with neuroblastoma and other solid tumors: a Children's Oncology Group study. *Pediatr. Blood Cancer* **55,** 629–638 (2010).
50 Weisenberger, D. J., Siegmund, K. D., Campan, M., Young, J., Long, T. I., Faasse, M. A. *et al.* CpG island methylator phenotype underlies sporadic microsatellite instability and is tightly associated with BRAF mutation in colorectal cancer. *Nat. Genet.* **38,** 787–793 (2006).

Published online 12 June 2013

Nucleic Acids Research, 2013, Vol. 41, No. 15 7231–7239
doi:10.1093/nar/gkt528

Visualization of multivalent histone modification in a single cell reveals highly concerted epigenetic changes on differentiation of embryonic stem cells

Naoko Hattori[1], Tohru Niwa[1], Kana Kimura[1], Kristian Helin[2,3] and Toshikazu Ushijima[1,*]

[1]Division of Epigenomics, National Cancer Center Research Institute, 5-1-1 Tsukiji, Chuo-ku, Tokyo 104-0045, Japan, [2]Biotech Research and Innovation Centre (BRIC), University of Copenhagen, Ole Maaløes Vej 5, 2200 Copenhagen, Denmark and [3]Centre for Epigenetics, University of Copenhagen, Ole Maaløes Vej 5, 2200 Copenhagen, Denmark

Received December 6, 2012; Revised May 19, 2013; Accepted May 22, 2013

ABSTRACT

Combinations of histone modifications have significant biological roles, such as maintenance of pluripotency and cancer development, but cannot be analyzed at the single cell level. Here, we visualized a combination of histone modifications by applying the *in situ* proximity ligation assay, which detects two proteins in close vicinity (~30 nm). The specificity of the method [designated as imaging of a combination of histone modifications (iChmo)] was confirmed by positive signals from H3K4me3/acetylated H3K9, H3K4me3/RNA polymerase II and H3K9me3/H4K20me3, and negative signals from H3K4me3/H3K9me3. Bivalent modification was clearly visualized by iChmo in wild-type embryonic stem cells (ESCs) known to have it, whereas rarely in *Suz12* knockout ESCs and mouse embryonic fibroblasts known to have little of it. iChmo was applied to analysis of epigenetic and phenotypic changes of heterogeneous cell population, namely, ESCs at an early stage of differentiation, and this revealed that the bivalent modification disappeared in a highly concerted manner, whereas phenotypic differentiation proceeded with large variations among cells. Also, using this method, we were able to visualize a combination of repressive histone marks in tissue samples. The application of iChmo to samples with heterogeneous cell population and tissue samples is expected to clarify unknown biological and pathological significance of various combinations of epigenetic modifications.

INTRODUCTION

Histone modifications are known to play important roles in various biological and pathological processes, such as cell type-specific gene expression and cancer development (1,2). In addition, the crucial importance of their combinations is indicated by recent findings, such as the presence of cell type-specific multivalent histone modifications revealed by genome-wide analyses (3–7) and proteins that recognize a combination of histone modifications (8). Especially, the combination of histone H3 lysine 4 trimethylation (H3K4me3) and histone H3 lysine 27 trimethylation (H3K27me3), named the bivalent modification, is present almost exclusively in pluripotent stem cells, such as embryonic stem cells (ESCs) (3,5), early stage embryos (9) and immature T-cells (10), and is thought to maintain the 'stemness' of these cells. Furthermore, aberrant expression of a protein that binds to a specific combination of histone modifications was associated with poor prognosis in breast cancer, suggesting the importance of a combination also in pathological processes (11).

Regardless of the crucial importance of combinations of histone modifications, methodologies to detect combinations are so far limited to the sequential-chromatin immunoprecipitation (sequential-ChIP) assay (3,12) and recently developed immunoprecipitation-mass spectrometry assay (13). Although a sequential-ChIP assay has the advantage to identify genomic regions with a specific combination of histone modifications, it suffers from the necessity of a large number of cells, and its application is limited to samples containing $>10^6$ cells. Moreover, in samples with heterogeneous cell populations, it is impossible to identify cells with a specific combination of histone modifications. Owing to this limitation, we cannot identify which cells have a specific multivalent

*To whom correspondence should be addressed. Tel: +81 3 3547 5240; Fax: +81 3 5565 1753; Email: tushijim@ncc.go.jp

modification in samples derived from tissues, and even in a cell line if the sample consists of cells at various differentiation stages.

In this study, we aimed to visualize the coexistence of two histone modifications by applying the *in situ* proximity ligation assay (*in situ* PLA), an imaging technique of protein–protein interactions (14). Based on the principle of *in situ* PLA, if two different modifications recognized by respective first antibodies exist approximately within 30 nm, oligonucleotide probes conjugated to their secondary antibodies can serve as a template for rolling-circle amplification. The amplification products can hybridize with fluorescent probes and be detected as fluorescence signals, reflecting the combination of histone modifications. In addition, we applied the method to analyze the presence of a specific combination of histone modifications in heterogeneous cell populations and tissue sections.

MATERIALS AND METHODS

Culture of mouse ESCs and embryonic fibroblasts

J1 ESC line and *Suz12* knockout (KO) ESC line (clone SBE8) established as reported (15) were cultured in normal ESC medium with 15% fetal bovine serum and 1000 U/ml of leukemia inhibitory factor (LIF) (ESGRO, Chemicon, CA) on mitotically inactivated mouse embryonic fibroblasts (MEFs) kindly provided by Dr Shiota K. (The University of Tokyo). For immunofluorescence staining and imaging of a combination of histone modifications (iChmo), MEFs at passage three were purchased from Millipore (Billerica, MA) and cultured in Dulbecco's modified Eagle's medium with 10% fetal bovine serum for 6 days at passage five. To induce differentiation of ESCs, cells were seeded on 0.1% gelatin-coated cell plate at a density of 3.0×10^5 cells/100 mm dish in the absence of feeder layer cells and LIF and then pre-cultured for 1 day. After pre-culture, ESCs were cultured for 24 or 48 h with 1 μM of all-trans retinoic acid (RA) (Sigma, St. Louis, MO). The medium was changed every day.

Preparation of mouse and human tissue samples

For RNA extraction, mouse liver and brain were resected from 8-week-old C57BL/6J male mice purchased from CLEA Japan, Inc. (Tokyo, Japan). For preparation of histological sections, human colonic tissues resected with a colon cancer were obtained, embedded in Tissue-Tek O.C.T. Compound (Sakura Finetek Japan, Tokyo, Japan) and frozen on dry ice. Sections of 4 μm of thickness were prepared for immunofluorescence staining and iChmo without a dry step. The animal experiments were approved by the Committee for Ethics in Animal Experimentation at the National Cancer Center. Human samples were obtained with informed consent, and the analysis was approved by the institutional review boards.

Immunofluorescence staining

For immunofluorescence staining, cells and tissue sections were fixed with 4% formaldehyde for 15 min, washed three times in PBS and permeabilized by 1% Triton X-100 in PBS for 20 min. After washing five times in PBS, cells and sections were incubated in blocking buffer (1% BSA in PBS) for 30 min and then with mouse monoclonal antibodies directed against H3K4me3 (1:1000; Wako, Tokyo, Japan; 307-34813), H4K20me3 (1:1000; Abcam, Cambridge, MA; ab78517), Oct-3/4 (1:500; Santa Cruz Biotechnology, Santa Cruz, CA; sc-5279) or ßIII-tubulin (1:500; Covance, Berkeley, CA; MMS-435P), or with rabbit polyclonal antibodies directed against acetylated H3K9 (H3K9ac) (1:500, Abcam; ab10812), H3K9me3 (1:1000, Millipore: 07-442), H3K27me3 (1:1000, Millipore; 07-449) or RNA polymerase II (RNAPII) (1:500, Abcam; ab5095) in the same buffer for 1 h. The specificity of antibodies against histone modifications was confirmed previously (16,17). Cells and sections were washed in PBS three times for 5 min and incubated in Alexa Fluor 594-conjugated goat anti-rabbit IgG (1:1000, Invitrogen, Carlsbad, CA) or Alexa Fluor 488-conjugated goat anti-mouse IgG (1:1000, Invitrogen) for 1 h. After washing with PBS three times for 5 min, coverslips were mounted using ProLong Gold antifade reagent with 4′,6-diamidino-2-phenylindole (DAPI) (Invitrogen). Fluorescence of cultured cells stained with histone modification antibodies was detected under a laser-scanning confocal microscope (LSM710; Carl Zeiss, Oberkochen, Germany), and all images were acquired and analyzed using LSM Software ZEN 2008 (Carl Zeiss). Images of Oct-4 and ßIII-tubulin staining of ESCs and of human tissue sections were captured using a FV10iW laser-scanning confocal microscope (Olympus, Tokyo, Japan).

iChmo

Duolink *in situ* PLA was purchased from Olink Bioscience (Uppsala, Sweden). First, cells and tissue sections were fixed, permeabilized and incubated with primary antibodies under the same condition in the immunofluorescence staining. The primary antibodies were the same as those for the immunofluorescence staining, and the concentrations were two times higher than those for the immunofluorescence staining. Then, samples were incubated with secondary antibodies conjugated with PLA probes MINUS and PLUS at 37°C for 90 min. Finally, the PLA probes MINUS and PLUS were ligated using two connecting oligonucleotides to produce a template for rolling-cycle amplification. After amplification, the amplification products were hybridized with red fluorescence-labeled oligonucleotide. Samples were mounted on coverslips using ProLong Gold antifade reagent with DAPI. Fluorescence of cultured cells was detected under LSM710, and all images were acquired and analyzed using ZEN 2008. For quantitative analysis of iChmo signals, the fluorescence spots were counted using Z-stack acquisition of BZ-9000 microscope system. Fluorescence of tissue sections was captured using a FV10iW laser-scanning confocal microscope.

Quantitative reverse transcription-PCR

DNase-treated total RNA (1 μg) was reverse-transcribed with Oligo-dT_{20} (Invitrogen, Carlsbad, CA) and Superscript III reverse transcriptase (Invitrogen).